

Understanding Multi-Granularity for Open-Vocabulary Part Segmentation

Jiho Choi^{1*}, Seonho Lee^{1*}, Seungho Lee², Minhyun Lee², Hyunjung Shim^{1†}

¹Graduate School of Artificial Intelligence, KAIST, Republic of Korea

²School of Integrated Technology, Yonsei University, Republic of Korea

{jihochoi, glanceeyes, kateshim}@kaist.ac.kr, {seungholee, lmh315}@yonsei.ac.kr

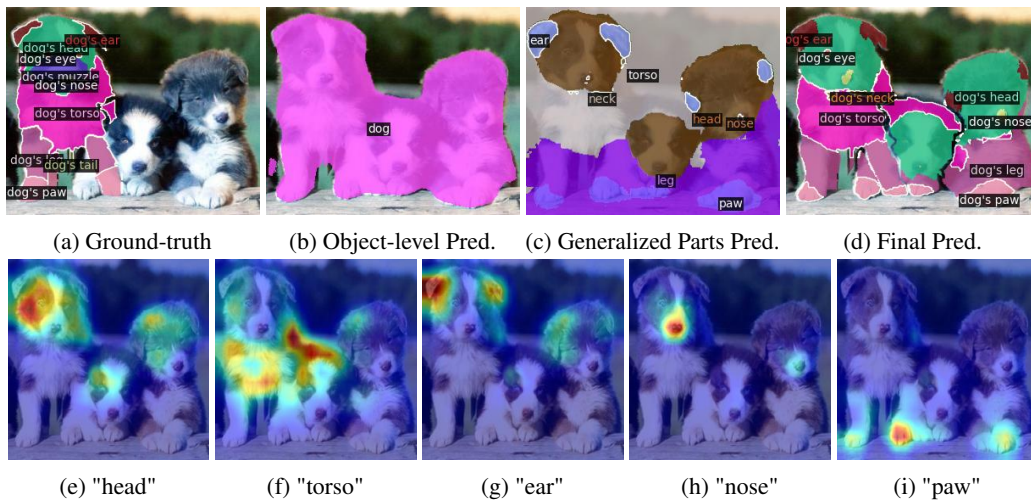


Figure 1: Prediction results of our PartCLIPSeg for unseen categories in the Pascal-Part-116 [7, 42] validation set. A “dog” is unseen during training. The final prediction of PartCLIPSeg utilizes (b) object-level context and (c) generalized parts, utilizing disjoint activation among (e)–(i) parts, and enhancing activation for smaller parts (e.g., (h) “nose”).

Abstract

Open-vocabulary part segmentation (OVPS) is an emerging research area focused on segmenting fine-grained entities based on diverse and previously unseen vocabularies. Our study highlights the inherent complexities of part segmentation due to intricate boundaries and diverse granularity, reflecting the knowledge-based nature of part identification. To address these challenges, we propose PartCLIPSeg, a novel framework utilizing generalized parts and object-level contexts to mitigate the lack of generalization in fine-grained parts. PartCLIPSeg integrates competitive part relationships and attention control techniques, alleviating ambiguous boundaries and underrepresented parts. Experimental results demonstrate that PartCLIPSeg outperforms existing state-of-the-art OVPS methods, offering refined segmentation and an advanced understanding of part relationships in images. Through extensive experiments, our model demonstrated an improvement over the state-of-the-art models on the Pascal-Part-116, ADE20K-Part-234, and PartImageNet datasets. Our code will be available at <https://github.com/kaist-cvml-lab/part-clipseg>.

*Both authors contributed equally to this work

†Corresponding author

1 Introduction

The pursuit of understanding parts and multi-granularity in computer vision [7, 19, 12] mirrors the innate complexities of animal instincts. For example, a “cheetah” instinctively targets an “impala’s neck” during a hunt, demonstrating its ability to distinguish specific parts. This ability extends to applications such as robot commands [40], image editing [28], and more sophisticated and fine-grained controls [41]. Part segmentation aims to mimic this ability by recognizing intricate details (e.g., parts) within objects, going beyond simple object-level segmentation to achieve detailed and diverse entity recognition.

Recognizing parts is more challenging than recognizing objects due to their complexity and diversity. Parts often have ambiguous boundaries not only defined by visual cues but also require a broader spectrum of information, reflecting their knowledge-based nature. For example, the “head” of a “dog” may include only the “face” or also the “neck” depending on the annotators’ perspective [7, 19].

To address difficulties in part segmentation, Open-Vocabulary Part Segmentation (OVPS) [36, 42, 40] has evolved by leveraging the knowledge of powerful Vision-Language Models (VLMs) like CLIP [34] or ALIGN [22]. Especially, it aims to achieve the adaptive recognition and processing of previously unseen categories with the aid of pre-trained VLMs, pushing the boundaries of vocabularies in traditional part segmentation. By utilizing Oracle supervision of base classes during training, recent studies in OVPS exploit part-level knowledge of base classes to generalize to novel classes. Recently, VLPART [36] uses DINO [5] features to map correspondences between base and novel classes and creates pseudo labels for novel categories. OV-PARTS [42] addresses the ambiguity of part boundaries by introducing object mask prompts and transferring knowledge of base class with few-shot approach. These methods successfully extract knowledge from VLMs and extend it to novel classes, achieving significant performance improvements in open-vocabulary settings.

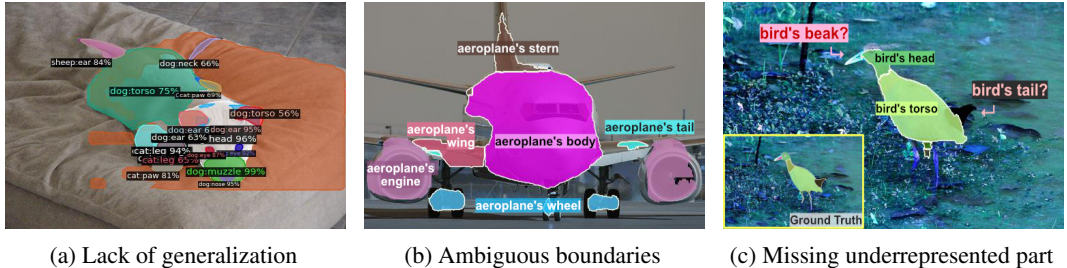


Figure 2: Limitations of existing OVPS methods in the prediction of unseen categories. (a) Lack of generalization: Classification of a “dog’s parts” involving categories like “cats” and “sheep”, “dog’s tail” misclassified as “sheep’s ear”. (VLPART [36]) (b) Ambiguous boundaries: Vague boundary output of “aeroplane’s body”. (c) Missing underrepresented parts: Neglect of parts such as “beak” and “leg”. (CLIPSeg [29, 42])

However, through empirical analysis of existing OVPS methods, we observed several common limitations in Figure 2. (Lack of generalization in (a)) Despite understanding part-level information, they often misidentify parts at the object level, e.g., a “dog’s leg” as a “cat’s leg”. Also, part-level misclassification occurs as the knowledge of parts in the base class fails to generalize to a novel class, e.g., “dog’s tail” as a “sheep’s ear”. (Ambiguous boundaries of parts in (b)) They fail to maintain non-overlapping relationships between parts, frequently resulting in overlaps, e.g., an “airplane’s wing” overlapping with its “body”. (Missing underrepresented parts in (c)) They ignore small and less frequent parts, causing prediction bias based on part size.

To overcome these limitations, we propose a novel framework called PartCLIPSeg, which consists of three main components. First, we devise generalized parts with object-level contexts to address the lack of generalization issue as the upper side of Figure 1. It explicitly obtains object-level and part-level pseudo-labels from VLMs and trains the OVPS model to satisfy both types of supervision. This guides the model to learn object boundaries while recognizing both part and object-level classes. Then, we suggest an attention control for minimizing the overlap between predicted parts, ensuring that parts are clearly separated as the lower side of Figure 1. In this way, we effectively leverage internal part information to learn ambiguous part boundaries. Finally, we enhance the activation related to certain parts by normalizing the activation scale of CLIP’s self-attention information. It

prevents small and less frequent areas from being ignored in pseudo-labels. This strategy ensures that the smallest granularity levels are retained in the final prediction. Through these three modules, PartCLIPSeg effectively addresses the challenges of existing OVPS methods and achieves robust multi-granularity segmentation. As a result, the proposed method achieves significant improvements in mIoU for both unseen and the harmonic mean compared to the previous state-of-the-art methods on Pascal-Part-116, ADE20K-Part-234, and PartImageNet in both Pred-All and Oracle-Obj settings.

2 Related Work

Open-Vocabulary Semantic Segmentation. Open vocabulary semantic segmentation (OVSS) goes beyond traditional semantic segmentation, which is restricted to predefined categories, by enabling predictions for unseen classes. Pioneering works focused on aligning predefined text embeddings with pixel-level visual features [4, 43, 49]. By leveraging large-scale Vision-Language Models (VLMs) like CLIP [34] and ALIGN [22], OVSS enables zero-shot segmentation through rich multi-modal features learned from extensive image-text pairs. MaskCLIP [51] modified CLIP’s image encoder to directly handle visual and text features for segmenting novel classes. Some works proposed two-stage strategy [14, 15, 17, 18, 26, 27, 46, 47]: first, models generate class-agnostic mask proposals [8, 9]; then, a pre-trained VLM predicts the category for each region. Some studies have introduced diffusion models to improve mask generation quality [46] or fine-tuned CLIP to enhance classification capabilities [18, 26]. Other studies have adopted a single-stage framework [10, 25, 29, 44, 48, 52]. They use pre-trained CLIP models to align pixel-level visual features with text features. ZegCLIP [52] enhances segmentation by incorporating learnable tokens. FC-CLIP [48] uses a frozen convolutional CLIP to predict class-agnostic masks and classifies using mask-pooled features [48]. CATSeg [10] and SED [44] generate pixel-level cost maps and refine them for segmentation. CLIPSeg [29] adds a lightweight transformer-based pixel decoder with a FiLM [16] module to fuse multi-modal features.

Part Segmentation. Part segmentation aims to identify individual parts of objects, a task that is more complex and costly due to the smaller and more diverse nature of parts compared to whole objects. To tackle this, various datasets like Pascal-Part [7], PartImageNet [19], ADE20k-Part [50], Cityscapes-Panoptic-Part [12], and PACO [2] provide diverse and detailed part annotations. Earlier studies [7, 21, 11, 39, 20] used self-supervised constraints and contrastive settings for effective part-level entity segmentation. Recent studies extended this to open-vocabulary scenarios [36, 31, 42], opening new avenues for handling diverse parts. By leveraging class-agnostic detectors [31] and Vision-Language Models like CLIP [36, 42], part segmentation has extended its generalization ability to unseen parts. Our work builds upon and extends methodologies from these studies.

3 Methodology

As illustrated in Figure 2, we identified three primary challenges of open-vocabulary part segmentation (OVPS): lack of generalization, overlapping parts, and missing underrepresented parts. Recognizing object-specific parts (such as “dog’s torso”) cannot be determined solely by looking at each part in isolation; it is imperative to consider both generalized part information and the overall context of the object. Furthermore, some parts may have overlapping meanings across different granularity labels (e.g., “eye”, “face”, and “head”). This implies that predictions should consider direct guidance for each part as well as the relationships between different parts. These intricate spatial and functional dependencies between parts are crucial for achieving a holistic understanding and precise predictions in fine-grained entity segmentation tasks.

Based on this motivation, we propose a novel OVPS method, PartCLIPSeg. This method leverages *generalized part information combined with object-level context* to tackle the lack of generalization problem (see Section 3.2). Also, we directly minimize the overlap among part predictions to improve the part boundaries (see Section 3.3.1). Finally, we normalize the scale of attention activation from various parts for handling missing underrepresented parts (see Section 3.3.2). The overall architecture of our method is shown in Figure 3.

3.1 Preliminary

OVPS aims to segment an image into a set of object-specific part categories $\mathbf{C}_{\text{obj-part}}^{\text{test}}$ (e.g., “dog’s head”, “car’s front”) in the *test* set, where the image is $\mathcal{I} \in \mathbb{R}^{H \times W \times 3}$, and H and W are the

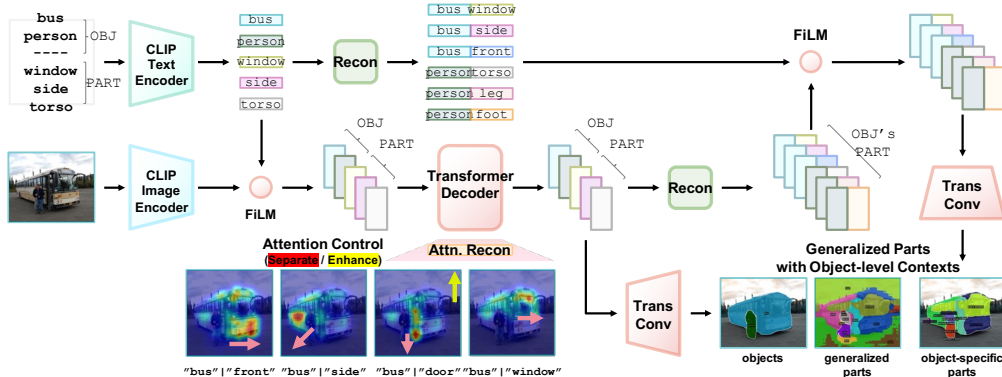


Figure 3: The overall architecture of PartCLIPSeg.

height and width. During training, image-mask pairs $\{(\mathcal{I}_k, \mathcal{M}_k)\}$ are used, consisting of images \mathcal{I}_k and corresponding ground-truth mask \mathcal{M}_k which only contains the object-specific part categories $\mathcal{C}_{\text{obj-part}}^{\text{train}}$ (e.g., “cat’s head,” “bus’s front”) in the *train* set.

Zero-Shot Part Segmentation. Open-vocabulary is a generalized zero-shot task, allowing the zero-shot segmentation protocol to evaluate zero-shot part segmentation performance. In this setting, *train* and *test* category names are divided into *seen* (base) and *unseen* (novel) sets, respectively, with disjoint object-specific category names; $\{\mathcal{C}_{\text{obj-part}}^{\text{unseen}} \cap \mathcal{C}_{\text{obj-part}}^{\text{seen}} = \emptyset\}$.

Cross-Dataset Setting. In this setting, the model is trained on one dataset and evaluated on another without fine-tuning. This means that the category names of *train* and *test* sets come from different datasets, denoted as $\mathcal{C}_{\text{obj-part}}^{\text{train}} \neq \mathcal{C}_{\text{obj-part}}^{\text{test}}$. Considering the domain gap between the datasets, this setting is more challenging.

3.2 Generalized Parts with Object-level Contexts

To address the lack of generalization problem, we propose leveraging generalized parts with object-level contexts. The concept of generalized parts involves identifying and utilizing common structural components that are shared across different object-level categories. For instance, many animals have parts like “head” or “torso” which, although functionally and visually distinct, may share certain underlying characteristics. By introducing generalized parts from object-specific parts, our PartCLIPSeg can efficiently recognize and segment these object-specific parts across diverse object classes, significantly enhancing the model’s ability to generalize from seen to unseen categories.

Although generalized parts help distinguish the part-level categories, the visual information of a part may not suffice for accurately classifying their object-level categories. For instance, predicting the “leg” part of an animal can be challenging to identify when solely examining the part as it may not clearly indicate to which animal it belongs. For this reason, there have been attempts to incorporate object-level guidance [36, 30, 42] in part segmentation. However, object-level guidance without a generalized part may lose contextual information and miss hierarchical relationships.

By integrating object contexts with generalized parts, PartCLIPSeg employs object-level guidance that captures the holistic essence of the object to which parts belong. This integration allows for a more precise understanding and classification of parts, improving the overall performance of OVPS.

Object and Part Embedding Generation. We modified the architecture from CLIPSeg [29, 42], which adopted CLIP [34] in encoder-decoder architecture for semantic segmentation. However, it is worth noting that our approach of utilizing generalized parts with object-level context is orthogonal to other previously proposed object-level segmentation methods [24, 5, 35].

The proposed approach begins by parsing an object-specific part category name, $c_{\text{obj-part}} \in \mathcal{C}_{\text{obj-part}}$, into separate components: an object category name (c_{obj}) and a generalized part category name (c_{part}), e.g., “cat” and “torso”. Then, CLIP text encoder, $\text{CLIP}_{\mathcal{T}}^*(\cdot)$, is used to transform these category names into their respective CLIP embeddings ($e_{\text{obj}}^{\mathcal{T}}$ and $e_{\text{part}}^{\mathcal{T}}$). It will condition the image features, $e^{\mathcal{I}}$, derived from CLIP image encoder, $\text{CLIP}_{\mathcal{I}}^*(\cdot)$ as:

$$e_{[\text{obj} | \text{part}]}^{\mathcal{T}} = \text{CLIP}_{\mathcal{T}}^*(c_{[\text{obj} | \text{part}]}) , e^{\mathcal{I}} = \text{CLIP}_{\mathcal{I}}^*(\mathcal{I}), \quad (1)$$

where $*$ denotes frozen pre-trained models. By using Feature-wise Linear Modulation (FiLM) [32, 38], each category name embeddings respectively modulate the image features as:

$$\mathbf{e}_{[\text{obj} | \text{part}] }^{\mathcal{I}} = \mathbf{e}^{\mathcal{I}} \oplus \text{FiLM}(\mathbf{e}_{[\text{obj} | \text{part}] }^{\mathcal{T}}), \quad (2)$$

where \oplus is an element-wise sum. FiLM is an adaptive affine transformation widely used for multi-modal or conditional tasks. It helps retrieve adequate conditioning for the image features. The modulated image features, $\mathbf{e}_{[\text{obj} | \text{part}] }^{\mathcal{I}}$, corresponding to each object and part category name, pass through a decoder module. The decoder module will be discussed in detail in Section 3.3. They then proceed through a transposed convolution model. Finally, the output mask of the object \hat{s}^o and part \hat{s}^p are evaluated with ground-truth mask of objects, s^o , and parts, s^p . Oracle supervision for the object and parts mask is simply computed from a combination of object-specific parts annotations: $s \in \mathcal{M}$.

Object-specific Part Construction. We utilize previously computed generalized part embeddings ($\mathbf{e}_{\text{part}}^{\mathcal{I}}, \mathbf{e}_{\text{part}}^{\mathcal{T}}$) and object embeddings ($\mathbf{e}_{\text{obj}}^{\mathcal{I}}, \mathbf{e}_{\text{obj}}^{\mathcal{T}}$) to reconstruct object-specific part embeddings. This process involves separate operations on modulated image features and category name embeddings.

Initially, we project the concatenated results of the object category name with the generalized part category name. This is to synthesize the embeddings for the target object-specific part category name. The approach ensures that the resultant embeddings are highly representative of parts and contextually relevant. The equivalent operation is applied to both object-level image features and part-level image features to generate object-specific image features as:

$$\mathbf{e}_{\text{obj-part}}^{[\mathcal{T}|\mathcal{I}]} = \text{Proj}(\left[\mathbf{e}_{\text{obj}}^{[\mathcal{T}|\mathcal{I}]} | \mathbf{e}_{\text{part}}^{[\mathcal{T}|\mathcal{I}]} \right]). \quad (3)$$

The resulting object-specific part embeddings are further refined by a FiLM process. Combined with the respective object-specific image features, final modulated object-specific part embeddings, $\mathbf{e}_{\text{obj-part}}^{\mathcal{I}}$ is computed as:

$$\mathbf{e}_{\text{obj-part}}^{\mathcal{I}} = \mathbf{e}_{\text{obj-part}}^{\mathcal{I}} \oplus \text{FiLM}(\mathbf{e}_{\text{obj-part}}^{\mathcal{T}}). \quad (4)$$

These embeddings are then processed through a deconvolution layer to produce the final segmentation masks $s \in \mathcal{M}$. This step ensures that the embeddings are precisely aligned to enhance the definition and accuracy of the object-specific part masks. It effectively bridges the gap between object and part-level categorical information with object-specific parts information.

Object, Part, and Object-specific Part Mask Supervision. The mask supervision is provided for three distinct categories: object-specific parts, objects, and generalized parts. This multi-faceted supervision enables our model to effectively disentangle generalized parts from objects, thereby facilitating a more nuanced learning process for OVPS. This disentanglement is crucial for the model to accurately recognize and differentiate between various object categories and their corresponding parts. It enhances the model’s ability to handle complex segmentation tasks with unseen object-specific parts. The overall mask guidance loss can be defined as follows:

$$\mathcal{L}_{\text{mask}} = \sum_{i=1}^{|\mathbf{C}_{\text{obj-part}}|+1} \underbrace{\{1 - \text{BCE}(s_i, \hat{s}_i)\}}_{\text{object-specific part}} + \lambda_1 \sum_{i=1}^{|\mathbf{C}_{\text{obj}}|+1} \underbrace{\{1 - \text{BCE}(s_i^o, \hat{s}_i^o)\}}_{\text{object guidance}} + \lambda_2 \sum_{i=1}^{|\mathbf{C}_{\text{part}}|} \underbrace{\{1 - \text{BCE}(s_i^p, \hat{s}_i^p)\}}_{\text{generalized part guidance}}, \quad (5)$$

where $|\mathbf{C}_{\text{obj-part}}| + 1$ and $|\mathbf{C}_{\text{obj}}| + 1$ are for uncategory (or background) prediction. The disentangled object and part generalization with object-specific parts guidance provides a clue to the lack of generalization problem.

3.3 Attention Control for Ambiguity and Omission

In this subsection, we address the previously mentioned challenges: (1) ambiguity in part boundaries and (2) omission of small or infrequently appearing parts. The main reason for these challenges is the incomplete guidance from knowledge-based, multi-granularity characteristics of parts. To overcome these, we adopt unsupervised methods traditionally used in fine-grained recognition and part discovery studies [7, 11, 39]. Specifically, we utilize approaches for adjusting self-attention activation inspired by the recent diffusion methods [37, 23, 6].

We assume that the distribution of self-attention activation maps for visual tokens belonging to the same object-specific part mask should exhibit inter-similarity characteristics [37], implying similar

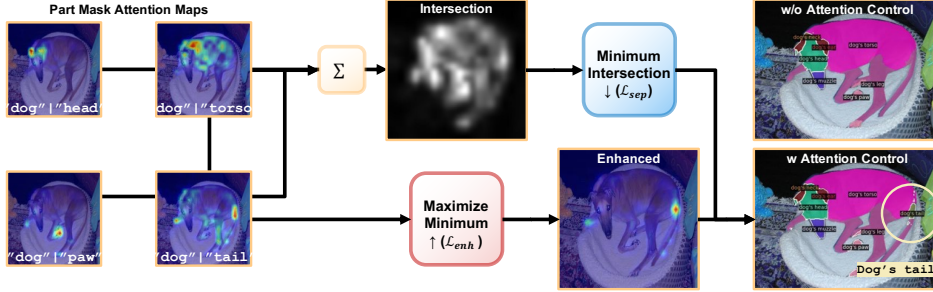


Figure 4: Example of Attention Control using Separation and Enhance losses. Our methods manipulates attention maps to accurately identify and segment small parts.

distributions. To this end, we first compute the average self-attention map $\mathcal{A}_{\mathcal{M}_c}$ for each object-specific part mask \mathcal{M}_c , where $c \in \mathbf{C}_{\text{obj-part}}$ represents an object-specific part category. This is done by summing the self-attention activation maps from channels specifically corresponding to object c_{obj} and part c_{part} , across all spatial tokens (h, w) within the mask, as follows:

$$\mathcal{A}_{\mathcal{M}_c} = \frac{1}{|\mathcal{M}_c|} \sum_{(h,w) \in \mathcal{M}_c} (\mathcal{A}_{c_{\text{obj}}}[h, w, :, :] + \mathcal{A}_{c_{\text{part}}}[h, w, :, :]). \quad (6)$$

Subsequently, the self-attention map $\mathcal{A}_{\mathcal{M}_c}$ for the object-specific part mask is refined through min-max normalization, followed by the application of a Gaussian filter to smooth the initial activation as in [6, 45]. Therefore, the dimensions of both the original and normalized self-attention maps for the object-specific part masks are as follows: $\mathcal{A}_{\mathcal{M}_c}, \mathcal{A}_{\mathcal{M}_c}^{\text{norm}} \in \mathbb{R}^{H \times W}$.

3.3.1 Minimizing Part Overlaps for Ambiguity

In the self-attention of the decoder layers, competition between object-specific parts helps define boundaries that cannot be sufficiently established by supervision alone. Using the previously obtained normalized attention map, our method generates parts with minimized intersections, inspired by [1, 3, 23, 33]. This approach effectively mitigates the ambiguity issue in part boundaries. Specifically, the normalized attention activation map $\mathcal{A}_{\mathcal{M}_c}^{\text{norm}}$ is first binarized based on an arbitrary threshold γ as:

$$\mathcal{B}_{\mathcal{M}_c}(h, w) = \mathbf{1}_{\{\mathcal{A}_{\mathcal{M}_c}^{\text{norm}}(h, w) \geq \gamma\}}. \quad (7)$$

where $\mathcal{B}_{\mathcal{M}_c}$ denotes binarized attention map for part mask \mathcal{M}_c . From now on, $\mathbf{C}_{\text{obj-part}}$ is simply denoted as \mathbf{C} . The separation loss \mathcal{L}_{sep} , which indicates the degree of intersection between object-specific parts, is as follows:

$$\mathcal{L}_{\text{sep}} = \frac{1}{|\mathbf{C}|} \left| \frac{\{(h, w) \mid \sum_{c \in \mathbf{C}} \mathcal{B}_{\mathcal{M}_c}(h, w) > 1\}}{\{(h, w) \mid \sum_{c \in \mathbf{C}} \mathcal{B}_{\mathcal{M}_c}(h, w) \geq 1\}} \right|, \quad (8)$$

where separating activation mitigates the challenge of ambiguous boundaries between parts.

3.3.2 Enhancing Part Activation for Omission

To address the omission problem, we employ a method inspired by attention controls in modern diffusion-based approaches [3, 6]. This approach enhances the activation within the self-attention activation map to enhance underrepresented parts before normalization. Specifically, for each object-specific part mask, the maximum value within the attention map is identified. Subsequently, among all object-specific parts, the minimum activation of the part with the maximum value is enhanced as:

$$\mathcal{L}_{\text{enh}} = 1 - \min_{c \in \mathbf{C}} \left(\max_{(h,w) \in \mathcal{M}_c} \mathcal{A}_{\mathcal{M}_c}[h, w] \right), \quad (9)$$

thereby boosting its representational efficacy. In this way, the enhance loss \mathcal{L}_{enh} provides sufficient guidance for small or infrequently occurring parts, effectively mitigating the omission problem.

Table 1: Comparison of zero-shot performance with state-of-the-art methods on Pascal-Part-116.

| Method | Backbone | Pred-All | | | Oracle-Obj | | |
|--------------------|------------|------------------|-------------------------|------------------------------------|------------------|-------------------------|------------------------------------|
| | | Seen | Unseen | Harmonic | Seen | Unseen | Harmonic |
| ZSSeg+ [47] | ResNet-50 | <u>54.31</u> | 16.08 | 24.71 | <u>54.43</u> | 19.04 | 28.21 |
| ZSSeg+ [47] | ResNet-101 | 56.87 | 20.29 | 29.91 | 57.88 | 21.93 | 31.81 |
| CATSeg [10] | ViT-B/16 | 41.65 | <u>26.08</u> | <u>32.07</u> | 43.97 | 26.11 | 32.76 |
| CLIPSeg [29, 42] | ViT-B/16 | 44.90 | 18.80 | 26.50 | 46.50 | <u>28.41</u> | <u>35.27</u> |
| PartCLIPSeg (ours) | ViT-B/16 | 44.37 \pm 0.43 | 27.29 \pm 0.21 | 33.79 \pm 0.08 (+1.72) | 50.02 \pm 0.50 | 31.67 \pm 0.27 | 38.79 \pm 0.11 (+3.52) |

¹ The best score is bold and the second-best score is underlined. The standard error of an average of 5 results is reported. These are the same for all experiments.

Table 2: Comparison of zero-shot performance with state-of-the-art methods on ADE20K-Part-234.

| Method | Backbone | Pred-All | | | Oracle-Obj | | |
|--------------------|------------|-------------------------|-------------------------|------------------------------------|------------------|-------------------------|------------------------------------|
| | | Seen | Unseen | Harmonic | Seen | Unseen | Harmonic |
| ZSSeg+ [47] | ResNet-50 | 21.30 | 5.60 | 8.87 | 43.19 | 27.84 | 33.85 |
| ZSSeg+ [47] | ResNet-101 | 21.42 | 3.30 | 5.76 | 43.41 | 25.70 | 32.28 |
| CATSeg [10] | ViT-B/16 | 20.23 | 8.27 | 11.74 | 31.40 | 25.77 | 28.31 |
| CLIPSeg [29, 42] | ViT-B/16 | <u>24.80</u> | 6.24 | 9.98 | 38.15 | <u>30.92</u> | <u>34.15</u> |
| PartCLIPSeg (ours) | ViT-B/16 | 30.89 \pm 0.53 | 14.39 \pm 0.07 | 19.63 \pm 0.07 (+7.89) | 38.37 \pm 0.14 | 38.82 \pm 0.25 | 38.60 \pm 0.07 (+4.45) |

The training objective for PartCLIPSeg integrates three key loss components as:

$$\mathcal{L}_{\text{all}} = \mathcal{L}_{\text{mask}} + \lambda_{\text{sep}}\mathcal{L}_{\text{sep}} + \lambda_{\text{enh}}\mathcal{L}_{\text{enh}}, \quad (10)$$

where (1) $\mathcal{L}_{\text{mask}}$ for generalized parts with object-level context, (2) \mathcal{L}_{sep} for addressing ambiguous boundaries, and (3) \mathcal{L}_{enh} for handling missing underrepresented parts.

4 Experiments

4.1 Experimental Setups

Datasets. We evaluate our method on three part segmentation datasets: Pascal part-116 [7, 42], ADE20K-Part-234 [50, 42], and PartImageNet [19]. Pascal-Part-116 [7, 42] consists of 8,431 training images and 850 test images. It is a modified version of PascalPart [7] by removing direction indicators for certain part classes and merging them to avoid overly complex part definitions. This dataset contains a total of 116 object part classes across 17 object categories. ADE20K-Part-234 [50, 42] consists of 7,347 training images and 1,016 validation images. It provides instance-level object mask annotations along with their corresponding part mask annotations, including 44 objects and 234 parts. PartImageNet [19] contains 16k training images and 2.9k validation images, segmented into 158 object classes from ImageNet [13] and organizes them into 11 super-categories. For our study, we select 40 object classes that represent common categories to assess cross-dataset performance effectively. More details about the datasets can be found in the supplementary materials.

Evaluation Protocols. We use two evaluation protocols for the performance of OVPS: (1) **Pred-All Setting**, where the ground truth mask and object class is not provided, and (2) **Oracle-Obj Setting**, where The ground truth mask and object class are known. In particular, the **Pred-Obj Setting** in OV-PARTS [42] uses predicted masks from off-the-shelf segmentation model. In contrast, our **Pred-All Setting** is a more challenging and practical setting because it does not rely on additional predicted masks or foundation models but solely uses the predicted object masks from the proposed model. For both evaluation protocols, we used mean Intersection over Union (mIoU) as an evaluation metric, which is widely used to measure segmentation performance.

Implementation Details. We build upon CLIPSeg [29, 42], a CLIP-based encoder-decoder model. The implementation details can be found in the supplementary material.

4.2 Performance Evaluation

Zero-Shot Part Segmentation. We compare our PartCLIPSeg to previous methods [47, 10, 29, 42] on three OVPS benchmarks [7, 50]. As shown in Table 1, PartCLIPSeg consistently outperforms

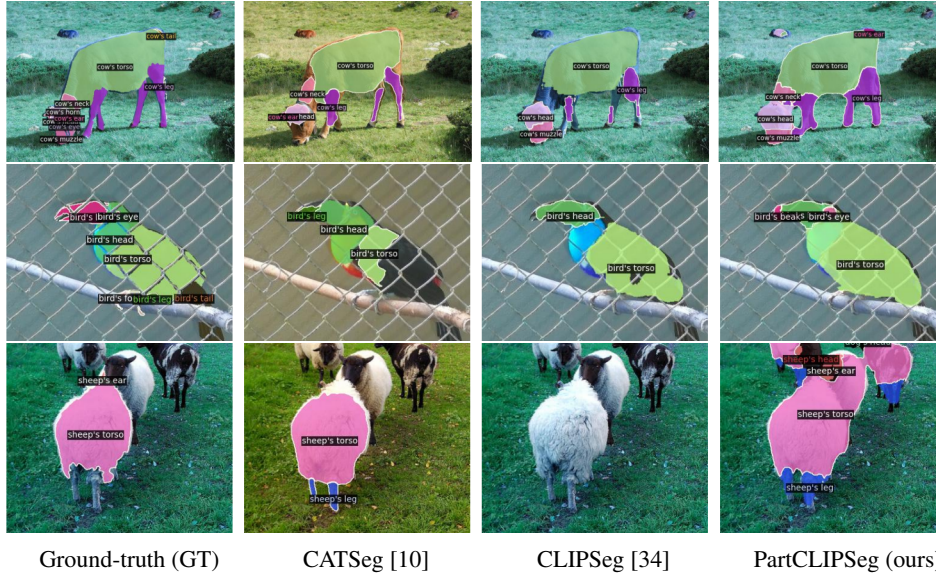


Figure 5: Qualitative results of zero-shot part segmentation on Pascal-Part-116 in Pred-All setting.

Table 3: Comparison of zero-shot performance with state-of-the-art method on PartImageNet.

| Method | Backbone | Pred-All | | | Oracle-Obj | | |
|--------------------|----------|-------------------------|-------------------------|------------------------------------|-------------------------|-------------------------|-------------------------------------|
| | | Seen | Unseen | Harmonic | Seen | Unseen | Harmonic |
| CLIPSeg [29, 42] | ViT-B/16 | 47.26 | 8.88 | 14.95 | 55.57 | 33.10 | 41.49 |
| PartCLIPSeg (ours) | ViT-B/16 | 41.70 \pm 0.74 | 21.97 \pm 0.45 | 28.75 \pm 0.30 (+13.8) | 57.16 \pm 0.30 | 52.31 \pm 0.62 | 54.62 \pm 0.37 (+13.13) |

previous approaches by significant margins on Pascal-Part-116, with improvements of 1.2% to 3.3% on unseen categories, demonstrating its generalization ability. Considering that performance in unseen categories is crucial in a zero-shot scenario, these results are significant despite some performance degradation in seen categories. Notably, the more challenging ADE20K-Part-234 dataset, which is a fine-grained segmentation dataset, further highlights the effectiveness of PartCLIPSeg. As shown in Table 2, PartCLIPSeg achieves a harmonic mean mIoU of 19.63% in the Pred-All setting, which is 7.89% higher than the best-performing baseline, and 38.60% in the Oracle-Obj setting, which is 4.45% higher than the best-performing baseline. We also evaluated PartCLIPSeg on PartImageNet. According to Table 3, PartCLIPSeg shows a notable improvement over CLIPSeg. In the Pred-All setting, we achieve a harmonic mean mIoU of 27.91%, a significant improvement of 12.96% over CLIPSeg’s 14.95%. In the Oracle-Obj setting, PartCLIPSeg achieves a harmonic mean mIoU of 53.95%, surpassing CLIPSeg by 12.46%.

We present the segmentation results of PartCLIPSeg in comparison to state-of-the-art open-vocabulary part segmentation methods [10, 29] on Pascal-Part-116. Specifically, we focus on qualitative performance on unseen categories such as “sheep” and “birds”. As shown in Figure 5, Our method effectively segments target parts without the need for predefined masks during inference. Notably, PartCLIPSeg excels at identifying smaller, often overlooked part classes. Additionally, our model manages to coherently segment multiple objects along with their respective parts, which can be challenging for other methods. These results demonstrate the effectiveness of PartCLIPSeg in zero-shot part segmentation across multiple benchmarks. Its improved performance on unseen categories and higher accuracy in challenging environments highlights the robustness and generalization capabilities of PartCLIPSeg. Consistent improvements on Pascal-Part-116, ADE20K-Part-234, and PartImageNet demonstrate that PartCLIPSeg sets a new standard in open-vocabulary part segmentation.

Cross-Dataset Part Segmentation. Table 4 validated the efficacy of our model in a cross-dataset setting, where category names, annotation style, and granularity of mask may vary. Additionally, unlike zero-shot situations within the same dataset, there are differences in the types and diversity of parts. Initially, we trained our model on PartImageNet [19]. Subsequent tests on Pascal-Part-116 [7, 42] showed that PartCLIPSeg significantly outperforms CLIPSeg in both the Pred-All and Oracle-Obj settings, confirming our model’s superiority on generalization in different datasets.

Table 5: Impact of Attention Control Losses

| Loss | | Pred-All | | | Oracle-Obj | | |
|---------------------|---------------------|--------------|--------------|--------------|--------------|--------------|--------------|
| \mathcal{L}_{sep} | \mathcal{L}_{enh} | Seen | Unseen | Harmonic | Seen | Unseen | Harmonic |
| Pascal-Part-116 | | | | | | | |
| ✗ | ✗ | 43.51 | 23.92 | 30.87 | 49.09 | 31.26 | 38.20 |
| ✓ | ✗ | 43.25 | 24.62 | 31.38 | 50.37 | 31.45 | 38.72 |
| ✓ | ✓ | 44.37 | 27.29 | 33.79 | <u>50.02</u> | 31.67 | 38.79 |
| ADE20K-Part-234 | | | | | | | |
| ✗ | ✗ | 28.00 | 14.84 | 19.40 | 37.39 | <u>36.49</u> | 36.93 |
| ✓ | ✗ | <u>30.83</u> | 14.27 | <u>19.51</u> | 39.46 | 36.04 | <u>37.67</u> |
| ✓ | ✓ | 30.89 | <u>14.39</u> | 19.63 | <u>38.37</u> | 38.82 | 38.60 |

Table 4: Cross-dataset performance

| Setting: PartImageNet \rightarrow Pascal-Part-116 | | |
|---|--------------|--------------|
| Method | Pred-All | Oracle-Obj |
| CLIPSeg | 14.09 | 14.87 |
| PartCLIPSeg (ours) | 16.49 | 19.86 |
| | (+2.40) | (+4.99) |

Table 6: Impact of PartCLIPSeg for small parts on Pascal-Part-116. PartCLIPSeg consistently outperforms CLIPSeg [29, 42] in most cases.

| | bird’s eye | cat’s eye | cow’s eye | dog’s eye | sheep’s eye | person’s eye |
|--------------------|--------------|--------------|--------------|--------------|--------------|---------------|
| CLIPSeg [29, 42] | 3.33 | 18.77 | 3.65 | 16.05 | 0.00 | 15.30 |
| PartCLIPSeg (ours) | 1.95 | 31.01 | 28.16 | 32.79 | 0.67 | 29.16 |
| | bird’s neck | cat’s neck | cow’s neck | dog’s neck | sheep’s neck | person’s neck |
| CLIPSeg [29, 42] | 19.09 | 6.57 | 0.78 | 8.12 | 8.47 | 30.93 |
| PartCLIPSeg (ours) | 32.51 | 12.00 | 2.75 | 16.37 | 18.80 | 50.71 |
| | bird’s leg | cat’s leg | cow’s leg | dog’s leg | sheep’s leg | person’s leg |
| CLIPSeg [29, 42] | 19.61 | 38.62 | 27.85 | 39.34 | 52.63 | 52.67 |
| PartCLIPSeg (ours) | 31.12 | 44.82 | 63.78 | 41.55 | 54.73 | 55.35 |

4.3 Ablation Study

In this section, we analyze the influence of different training losses on PartCLIPSeg. We focus on the roles of separation and enhance losses, examining how they contribute to improved segmentation accuracy.

Separation & Enhance Losses. We conducted an ablation study to investigate the effect of the separation loss \mathcal{L}_{sep} and the enhance loss \mathcal{L}_{enh} on PartCLIPSeg performance in Table 5). On Pascal-Part-116, eliminating both losses resulted in a lower harmonic mean (30.87) in Pred-All and a harmonic mean of 38.20 in Oracle-Obj. Introducing \mathcal{L}_{sep} without \mathcal{L}_{enh} improved the harmonic mean to 31.38 in Pred-All and 38.72 in Oracle-Obj. Using both losses resulted in the highest harmonic means of 33.79 and 38.79, respectively. Similarly, for ADE20K-Part-234, using both losses resulted in the best performance, with harmonic means of 19.63 in Pred-All and 38.60 in Oracle-Obj. These results highlight the crucial role of both separation and enhance losses in improving performance.

Impact of PartCLIPSeg for Underrepresented Parts. We investigate the effect of the enhance loss \mathcal{L}_{enh} on OVPS model performance, especially with respect to underrepresented parts. In Table 6, we compare our PartCLIPSeg with CLIPSeg [29, 42] on Pascal-Part-116. The results demonstrate that our method significantly improves its ability to recognize underrepresented parts compared to CLIPSeg. For example, our method achieves an IoU of 28.16 for the “cow’s eye” compared to CLIPSeg’s 3.65 and 32.79 for the “dog’s eye” compared to CLIPSeg’s 16.05. Similarly, for the “bird’s neck”, PartCLIPSeg shows an IoU of 32.51, significantly higher than CLIPSeg’s 19.09. These improvements highlight the effectiveness of the enhance loss in accurately segmenting small and intricate parts, demonstrating its crucial role in improving the overall performance.

5 Conclusion

In this study, we introduced PartCLIPSeg, a state-of-the-art OVPS method that addresses three primary challenges in OVPS. PartCLIPSeg utilizes generalized parts and object-level guidance to effectively solve identification issues. Then, it separates parts by minimizing their overlaps in attention maps, thus learning ambiguous part boundaries. Additionally, we implemented an enhanced loss function to improve the detection of underrepresented parts. Through extensive experimentation, we have confirmed the superior performance of PartCLIPSeg.

References

- [1] Aishwarya Agarwal, Srikrishna Karanam, KJ Joseph, Apoorv Saxena, Koustava Goswami, and Balaji Vasan Srinivasan. A-star: Test-time attention segregation and retention for text-to-image synthesis. In *Proceedings of the IEEE/CVF International Conference on Computer Vision*, pages 2283–2293, 2023.
- [2] Juan Antonio Balbuena, Raúl Míguez-Lozano, and Isabel Blasco-Costa. Paco: a novel procrustes application to cophylogenetic analysis. *PLoS one*, 8(4):e61048, 2013.
- [3] Zhipeng Bao, Yijun Li, Krishna Kumar Singh, Yu-Xiong Wang, and Martial Hebert. Separate-and-enhance: Compositional finetuning for text2image diffusion models. *arXiv preprint arXiv:2312.06712*, 2023.
- [4] Maxime Bucher, Tuan-Hung Vu, Matthieu Cord, and Patrick Pérez. Zero-shot semantic segmentation. *Advances in Neural Information Processing Systems*, 32, 2019.
- [5] Mathilde Caron, Hugo Touvron, Ishan Misra, Hervé Jégou, Julien Mairal, Piotr Bojanowski, and Armand Joulin. Emerging properties in self-supervised vision transformers. In *Proceedings of the IEEE/CVF international conference on computer vision*, pages 9650–9660, 2021.
- [6] Hila Chefer, Yuval Alaluf, Yael Vinker, Lior Wolf, and Daniel Cohen-Or. Attend-and-excite: Attention-based semantic guidance for text-to-image diffusion models. *ACM Transactions on Graphics (TOG)*, 42(4):1–10, 2023.
- [7] Xianjie Chen, Roozbeh Mottaghi, Xiaobai Liu, Sanja Fidler, Raquel Urtasun, and Alan Yuille. Detect what you can: Detecting and representing objects using holistic models and body parts. In *Proceedings of the IEEE conference on computer vision and pattern recognition*, pages 1971–1978, 2014.
- [8] Bowen Cheng, Alex Schwing, and Alexander Kirillov. Per-pixel classification is not all you need for semantic segmentation. *Advances in neural information processing systems*, 34: 17864–17875, 2021.
- [9] Bowen Cheng, Ishan Misra, Alexander G Schwing, Alexander Kirillov, and Rohit Girdhar. Masked-attention mask transformer for universal image segmentation. In *Proceedings of the IEEE/CVF conference on computer vision and pattern recognition*, pages 1290–1299, 2022.
- [10] Seokju Cho, Heeseong Shin, Sunghwan Hong, Seungjun An, Seungjun Lee, Anurag Arnab, Paul Hongsuck Seo, and Seungryong Kim. Cat-seg: Cost aggregation for open-vocabulary semantic segmentation. *arXiv preprint arXiv:2303.11797*, 2023.
- [11] Subhabrata Choudhury, Iro Laina, Christian Rupprecht, and Andrea Vedaldi. Unsupervised part discovery from contrastive reconstruction. *Advances in Neural Information Processing Systems*, 34:28104–28118, 2021.
- [12] Daan de Geus, Panagiotis Meletis, Chenyang Lu, Xiaoxiao Wen, and Gijs Dubbelman. Part-aware panoptic segmentation. In *Proceedings of the IEEE/CVF Conference on Computer Vision and Pattern Recognition*, pages 5485–5494, 2021.
- [13] Jia Deng, Wei Dong, Richard Socher, Li-Jia Li, Kai Li, and Li Fei-Fei. Imagenet: A large-scale hierarchical image database. In *2009 IEEE conference on computer vision and pattern recognition*, pages 248–255. Ieee, 2009.
- [14] Jian Ding, Nan Xue, Gui-Song Xia, and Dengxin Dai. Decoupling zero-shot semantic segmentation. In *Proceedings of the IEEE/CVF Conference on Computer Vision and Pattern Recognition*, pages 11583–11592, 2022.
- [15] Zheng Ding, Jieke Wang, and Zhuowen Tu. Open-vocabulary universal image segmentation with maskclip. *arXiv preprint arXiv:2208.08984*, 2022.
- [16] Vincent Dumoulin, Ethan Perez, Nathan Schucher, Florian Strub, Harm de Vries, Aaron Courville, and Yoshua Bengio. Feature-wise transformations. *Distill*, 3(7):e11, 2018.

- [17] Golnaz Ghiasi, Xiuye Gu, Yin Cui, and Tsung-Yi Lin. Scaling open-vocabulary image segmentation with image-level labels. In *European Conference on Computer Vision*, pages 540–557. Springer, 2022.
- [18] Kunyang Han, Yong Liu, Jun Hao Liew, Henghui Ding, Jiajun Liu, Yitong Wang, Yansong Tang, Yujiu Yang, Jiashi Feng, Yao Zhao, et al. Global knowledge calibration for fast open-vocabulary segmentation. In *Proceedings of the IEEE/CVF International Conference on Computer Vision*, pages 797–807, 2023.
- [19] Ju He, Shuo Yang, Shaokang Yang, Adam Kortylewski, Xiaoding Yuan, Jie-Neng Chen, Shuai Liu, Cheng Yang, Qihang Yu, and Alan Yuille. Partimagenet: A large, high-quality dataset of parts. In *European Conference on Computer Vision*, pages 128–145. Springer, 2022.
- [20] Ju He, Jieneng Chen, Ming-Xian Lin, Qihang Yu, and Alan L Yuille. Compositor: Bottom-up clustering and compositing for robust part and object segmentation. In *Proceedings of the IEEE/CVF Conference on Computer Vision and Pattern Recognition*, pages 11259–11268, 2023.
- [21] Wei-Chih Hung, Varun Jampani, Sifei Liu, Pavlo Molchanov, Ming-Hsuan Yang, and Jan Kautz. Scops: Self-supervised co-part segmentation. In *Proceedings of the IEEE/CVF Conference on Computer Vision and Pattern Recognition*, pages 869–878, 2019.
- [22] Chao Jia, Yinfei Yang, Ye Xia, Yi-Ting Chen, Zarana Parekh, Hieu Pham, Quoc Le, Yun-Hsuan Sung, Zhen Li, and Tom Duerig. Scaling up visual and vision-language representation learning with noisy text supervision. In *International conference on machine learning*, pages 4904–4916. PMLR, 2021.
- [23] Yunji Kim, Jiyoung Lee, Jin-Hwa Kim, Jung-Woo Ha, and Jun-Yan Zhu. Dense text-to-image generation with attention modulation. In *Proceedings of the IEEE/CVF International Conference on Computer Vision*, pages 7701–7711, 2023.
- [24] Alexander Kirillov, Eric Mintun, Nikhila Ravi, Hanzi Mao, Chloe Rolland, Laura Gustafson, Tete Xiao, Spencer Whitehead, Alexander C Berg, Wan-Yen Lo, et al. Segment anything. In *Proceedings of the IEEE/CVF International Conference on Computer Vision*, pages 4015–4026, 2023.
- [25] Boyi Li, Kilian Q Weinberger, Serge Belongie, Vladlen Koltun, and René Ranftl. Language-driven semantic segmentation. *arXiv preprint arXiv:2201.03546*, 2022.
- [26] Feng Liang, Bichen Wu, Xiaoliang Dai, Kunpeng Li, Yinan Zhao, Hang Zhang, Peizhao Zhang, Peter Vajda, and Diana Marculescu. Open-vocabulary semantic segmentation with mask-adapted clip. In *Proceedings of the IEEE/CVF Conference on Computer Vision and Pattern Recognition*, pages 7061–7070, 2023.
- [27] Yong Liu, Sule Bai, Guanbin Li, Yitong Wang, and Yansong Tang. Open-vocabulary segmentation with semantic-assisted calibration. *arXiv preprint arXiv:2312.04089*, 2023.
- [28] Zongdai Liu, Feixiang Lu, Peng Wang, Hui Miao, Liangjun Zhang, Ruigang Yang, and Bin Zhou. 3d part guided image editing for fine-grained object understanding. In *Proceedings of the IEEE/CVF Conference on Computer Vision and Pattern Recognition*, pages 11336–11345, 2020.
- [29] Timo Lüddecke and Alexander Ecker. Image segmentation using text and image prompts. In *Proceedings of the IEEE/CVF conference on computer vision and pattern recognition*, pages 7086–7096, 2022.
- [30] Umberto Michieli and Pietro Zanuttigh. Edge-aware graph matching network for part-based semantic segmentation. *International Journal of Computer Vision*, 130(11):2797–2821, 2022.
- [31] Tai-Yu Pan, Qing Liu, Wei-Lun Chao, and Brian Price. Towards open-world segmentation of parts. In *Proceedings of the IEEE/CVF Conference on Computer Vision and Pattern Recognition*, pages 15392–15401, 2023.

- [32] Ethan Perez, Florian Strub, Harm De Vries, Vincent Dumoulin, and Aaron Courville. Film: Visual reasoning with a general conditioning layer. In *Proceedings of the AAAI conference on artificial intelligence*, volume 32, 2018.
- [33] Quynh Phung, Songwei Ge, and Jia-Bin Huang. Grounded text-to-image synthesis with attention refocusing. *arXiv preprint arXiv:2306.05427*, 2023.
- [34] Alec Radford, Jong Wook Kim, Chris Hallacy, Aditya Ramesh, Gabriel Goh, Sandhini Agarwal, Girish Sastry, Amanda Askell, Pamela Mishkin, Jack Clark, et al. Learning transferable visual models from natural language supervision. In *International conference on machine learning*, pages 8748–8763. PMLR, 2021.
- [35] Tianhe Ren, Shilong Liu, Ailing Zeng, Jing Lin, Kunchang Li, He Cao, Jiayu Chen, Xinyu Huang, Yukang Chen, Feng Yan, et al. Grounded sam: Assembling open-world models for diverse visual tasks. *arXiv preprint arXiv:2401.14159*, 2024.
- [36] Peize Sun, Shoufa Chen, Chenchen Zhu, Fanyi Xiao, Ping Luo, Saining Xie, and Zhicheng Yan. Going denser with open-vocabulary part segmentation. In *Proceedings of the IEEE/CVF International Conference on Computer Vision*, pages 15453–15465, 2023.
- [37] Junjiao Tian, Lavisha Aggarwal, Andrea Colaco, Zsolt Kira, and Mar Gonzalez-Franco. Diffuse, attend, and segment: Unsupervised zero-shot segmentation using stable diffusion. *arXiv preprint arXiv:2308.12469*, 2023.
- [38] Mehmet Ozgur Turkoglu, Alexander Becker, Hüseyin Anil Gündüz, Mina Rezaei, Bernd Bischl, Rodrigo Caye Daudt, Stefano D’Aronco, Jan Wegner, and Konrad Schindler. Film-ensemble: probabilistic deep learning via feature-wise linear modulation. *Advances in neural information processing systems*, 35:22229–22242, 2022.
- [39] Robert van der Klis, Stephan Alaniz, Massimiliano Mancini, Cassio F Dantas, Dino Ienco, Zeynep Akata, and Diego Marcos. Pdisconet: Semantically consistent part discovery for fine-grained recognition. In *Proceedings of the IEEE/CVF International Conference on Computer Vision*, pages 1866–1876, 2023.
- [40] Zifu Wan, Yaqi Xie, Ce Zhang, Zhiqiu Lin, Zihan Wang, Simon Stepputtis, Deva Ramanan, and Katia P Sycara. Instructpart: Affordance-based part segmentation from language instruction. In *AAAI-2024 Workshop on Public Sector LLMs: Algorithmic and Sociotechnical Design*, 2024.
- [41] Xudong Wang, Trevor Darrell, Sai Saketh Rambhatla, Rohit Girdhar, and Ishan Misra. Instancediffusion: Instance-level control for image generation. *arXiv preprint arXiv:2402.03290*, 2024.
- [42] Meng Wei, Xiaoyu Yue, Wenwei Zhang, Shu Kong, Xihui Liu, and Jiangmiao Pang. Ov-parts: Towards open-vocabulary part segmentation. *Advances in Neural Information Processing Systems*, 36, 2024.
- [43] Yongqin Xian, Subhabrata Choudhury, Yang He, Bernt Schiele, and Zeynep Akata. Semantic projection network for zero-and few-label semantic segmentation. In *Proceedings of the IEEE/CVF Conference on Computer Vision and Pattern Recognition*, pages 8256–8265, 2019.
- [44] Bin Xie, Jiale Cao, Jin Xie, Fahad Shahbaz Khan, and Yanwei Pang. Sed: A simple encoder-decoder for open-vocabulary semantic segmentation. *arXiv preprint arXiv:2311.15537*, 2023.
- [45] Jinheng Xie, Yuexiang Li, Yawen Huang, Haozhe Liu, Wentian Zhang, Yefeng Zheng, and Mike Zheng Shou. Boxdiff: Text-to-image synthesis with training-free box-constrained diffusion. In *Proceedings of the IEEE/CVF International Conference on Computer Vision*, pages 7452–7461, 2023.
- [46] Jiarui Xu, Sifei Liu, Arash Vahdat, Wonmin Byeon, Xiaolong Wang, and Shalini De Mello. Open-vocabulary panoptic segmentation with text-to-image diffusion models. In *Proceedings of the IEEE/CVF Conference on Computer Vision and Pattern Recognition*, pages 2955–2966, 2023.

- [47] Mengde Xu, Zheng Zhang, Fangyun Wei, Yutong Lin, Yue Cao, Han Hu, and Xiang Bai. A simple baseline for open-vocabulary semantic segmentation with pre-trained vision-language model. In *European Conference on Computer Vision*, pages 736–753. Springer, 2022.
- [48] Qihang Yu, Ju He, Xueqing Deng, Xiaohui Shen, and Liang-Chieh Chen. Convolutions die hard: Open-vocabulary segmentation with single frozen convolutional clip. *Advances in Neural Information Processing Systems*, 36, 2024.
- [49] Hang Zhao, Xavier Puig, Bolei Zhou, Sanja Fidler, and Antonio Torralba. Open vocabulary scene parsing. In *Proceedings of the IEEE International Conference on Computer Vision*, pages 2002–2010, 2017.
- [50] Bolei Zhou, Hang Zhao, Xavier Puig, Sanja Fidler, Adela Barriuso, and Antonio Torralba. Scene parsing through ade20k dataset. In *Proceedings of the IEEE conference on computer vision and pattern recognition*, pages 633–641, 2017.
- [51] Chong Zhou, Chen Change Loy, and Bo Dai. Extract free dense labels from clip. In *European Conference on Computer Vision*, pages 696–712. Springer, 2022.
- [52] Ziqin Zhou, Yinjie Lei, Bowen Zhang, Lingqiao Liu, and Yifan Liu. Zegclip: Towards adapting clip for zero-shot semantic segmentation. In *Proceedings of the IEEE/CVF Conference on Computer Vision and Pattern Recognition*, pages 11175–11185, 2023.